

This article was downloaded by:

On: 23 January 2011

Access details: *Access Details: Free Access*

Publisher *Taylor & Francis*

Informa Ltd Registered in England and Wales Registered Number: 1072954 Registered office: Mortimer House, 37-41 Mortimer Street, London W1T 3JH, UK



## Journal of Liquid Chromatography & Related Technologies

Publication details, including instructions for authors and subscription information:

<http://www.informaworld.com/smpp/title~content=t713597273>

### Thermodynamic and Kinetic Characterization of Porous Graphitic Carbon in Reversed-Phase Liquid Chromatography

Yuening Zhang<sup>a</sup>; Victoria L. McGuffin<sup>a</sup>

<sup>a</sup> Department of Chemistry, Michigan State University, East Lansing, Michigan, USA

**To cite this Article** Zhang, Yuening and McGuffin, Victoria L.(2007) 'Thermodynamic and Kinetic Characterization of Porous Graphitic Carbon in Reversed-Phase Liquid Chromatography', *Journal of Liquid Chromatography & Related Technologies*, 30: 11, 1551 – 1575

**To link to this Article:** DOI: 10.1080/10826070701221396

**URL:** <http://dx.doi.org/10.1080/10826070701221396>

PLEASE SCROLL DOWN FOR ARTICLE

Full terms and conditions of use: <http://www.informaworld.com/terms-and-conditions-of-access.pdf>

This article may be used for research, teaching and private study purposes. Any substantial or systematic reproduction, re-distribution, re-selling, loan or sub-licensing, systematic supply or distribution in any form to anyone is expressly forbidden.

The publisher does not give any warranty express or implied or make any representation that the contents will be complete or accurate or up to date. The accuracy of any instructions, formulae and drug doses should be independently verified with primary sources. The publisher shall not be liable for any loss, actions, claims, proceedings, demand or costs or damages whatsoever or howsoever caused arising directly or indirectly in connection with or arising out of the use of this material.

## Thermodynamic and Kinetic Characterization of Porous Graphitic Carbon in Reversed-Phase Liquid Chromatography

Yuening Zhang and Victoria L. McGuffin

Department of Chemistry, Michigan State University, East Lansing,  
Michigan, USA

**Abstract:** The thermodynamics and kinetics of solute transfer on porous graphitic carbon (PGC) are studied for two series of aromatic hydrocarbons, alkylbenzenes and methylbenzenes. The retention behavior is characterized as a function of temperature, pressure, length of alkyl chain, and number and position of methyl substituents. In the thermodynamic studies, the retention factor ( $k$ ) increases with an increase in the length of alkyl chain or number of methyl substituents. The data indicate that increases in the number of methylene and methyl substituents result in more negative changes in molar enthalpy ( $\Delta H_{sm}$ ). Hence, the transition from mobile to stationary phase is a more energetically favorable, exothermic process with each methylene or methyl group added. The data also show that the change in molar volume ( $\Delta V_{sm}$ ) is close to zero, which is consistent with an adsorption mechanism on PGC. Enthalpy-entropy compensation is observed for both homologous series, and the compensation temperature suggests that the retention mechanism is distinctly different for the methylene and methyl groups. In the kinetic studies, the rate of solute transfer increases with an increasing number of methylene and methyl groups. The activation enthalpy from the stationary phase to transition state ( $\Delta H_{\ddagger s}$ ) is found to increase with an increasing number of methylene and methyl groups. But the activation enthalpy from the mobile phase to transition state ( $\Delta H_{\ddagger m}$ ) is much smaller than  $\Delta H_{\ddagger s}$  and, at the same time, is very similar for all the solutes. The activation volumes ( $\Delta V_{\ddagger s}$  and  $\Delta V_{\ddagger m}$ ) are very close to zero, again owing to the adsorption mechanism on PGC. These results demonstrate that the retention mechanism for PGC, which is based on adsorption, is

Address correspondence to Victoria L. McGuffin, Department of Chemistry, Michigan State University, East Lansing, Michigan 48824-1322, USA. E-mail: jgshabus@aol.com

different from that for octadecylsilica, the most widely used stationary phase in liquid chromatography.

**Keywords:** Thermodynamics, Kinetics, Porous graphitic carbon, Reversed-phase liquid chromatography, Alkylbenzenes, Methylbenzenes

## INTRODUCTION

Porous graphitic carbon (PGC) is a very attractive stationary phase for reversed-phase liquid chromatography.<sup>[1]</sup> It is produced from a silica template, which is impregnated with phenol and hexylamine and heated gradually to 150°C. This silica-polymer is heated to 900°C in nitrogen, then treated with aqueous potassium hydroxide to dissolve the silica template. The remaining carbonaceous material is heated to 2,500°C in argon. The final product is a two dimensional form of graphite with a unique sponge-like structure, which gives it good mechanical strength while maintaining sufficient surface area and porosity. Graphite is a crystalline material made up of sheets containing hexagonally arranged carbon atoms linked by aromatic (1.5 order) bonds. There are, in principle, no adventitious functional groups on the surface because the aromatic carbon atoms have all valencies satisfied. Perfect graphite is, therefore, an intrinsically reproducible material with a completely uniform surface, free from any functional groups.<sup>[2]</sup> Furthermore, graphite is one of the most unreactive substances known and can withstand any mobile phase that will not attack the chromatographic equipment itself.<sup>[1]</sup>

Porous graphitic carbon can achieve separations of nonpolar,<sup>[3]</sup> polar,<sup>[4]</sup> and ionized organic compounds,<sup>[5]</sup> as well as geometric and positional isomers.<sup>[6]</sup> A number of very unusual separations can be successfully performed with PGC as stationary phase. These separations are difficult or impossible with more conventional reversed-phase materials, such as octadecylsilica or polystyrene-divinylbenzene polymers. Although significant efforts have been invested in the applications of PGC in both chromatography and extraction, the retention mechanism is far from being understood. Limitations in both theory and experimental design have hindered definitive quantitative analysis. The investigations of molecular contributions to retention on PGC have been limited primarily to retention and selectivity factors.<sup>[7,8]</sup> Virtually no studies have sought to characterize the change in molar enthalpy and molar volume, which provide insight into how molecules interact with the stationary phase. In addition to thermodynamic information, the kinetics of retention have also been largely overlooked. The kinetics of retention are important because they provide insight into the rate at which transitions occur, as well as the energy barriers that exist for a molecule to transfer from one phase to another. A detailed thermodynamic and kinetic study will help to understand and characterize the retention mechanism of PGC.

## THEORY

In order to characterize the solutes undergoing adsorption on the PGC stationary phase, it is necessary to utilize a theoretical approach by which they can be compared. The relationships of chemical thermodynamics and kinetics provide such an approach.<sup>[9-11]</sup> The thermodynamic parameters describe the path-independent measures of solute transfer from mobile to stationary phase. These parameters are calculated from the retention factor ( $k$ ), which is a function of the retention times of the solute ( $t_r$ ) as well as a nonretained compound ( $t_0$ )

$$k = \frac{t_r - t_0}{t_0} \quad (1)$$

The retention factor can be related to the changes in molar enthalpy ( $\Delta H$ ) and molar entropy ( $\Delta S$ ) through the van't Hoff equation

$$\ln k = \frac{-\Delta H}{RT} + \frac{\Delta S}{R} - \ln \beta \quad (2)$$

where  $R$  is the gas constant,  $T$  the absolute temperature, and  $\beta$  the phase ratio. This equation allows for the calculation of  $\Delta H$  from the slope of a graph of  $\ln k$  versus  $1/T$  at constant pressure. The intercept contains information about the change in molar entropy as well as the phase ratio, which is the ratio of the volume of mobile and stationary phases. Because the phase ratio is not accurately known, the change in molar entropy cannot be reliably calculated. The retention factor can be related to the pressure ( $P$ ) by

$$\ln k = \frac{(-\Delta E + T\Delta S - P\Delta V)}{RT} - \ln \beta \quad (3)$$

where  $\Delta E$  is the change in molar internal energy and  $\Delta V$  is the change in molar volume. This equation allows for the calculation of  $\Delta V$  from the slope of a graph of  $\ln k$  versus  $P$  at constant temperature.

To gain a greater understanding of the balance of thermodynamic contributions to solute retention, enthalpy-entropy compensation is very useful.<sup>[12,13]</sup> For a homologous series of solutes that obey a linear free energy relationship, there exists a hypothetical temperature at which the relative changes in enthalpy and entropy are balanced and the net change in free energy is zero. The retention factor can be related to the change in free energy ( $\Delta G$ ) at the compensation temperature ( $T_c$ ) by

$$\ln k = \frac{-\Delta H}{R} \left( \frac{1}{T} - \frac{1}{T_c} \right) + \frac{\Delta G_{T_c}}{RT_c} - \ln \beta \quad (4)$$

Thus, a graph of the natural logarithm of the retention factor versus the change in molar enthalpy may be used to evaluate enthalpy-entropy compensation. If compensation occurs, this graph will be linear and the slope can be used to

calculate the compensation temperature. The compensation temperature may be used to compare the retention mechanisms for different solutes, different mobile phases, or different stationary phases. As discussed by Ranatunga et al.,<sup>[14]</sup> if the compensation temperatures are identical, then the relative contributions of enthalpy and entropy to the overall free energy are the same for the two systems. However, if the compensation temperatures are different, then the underlying retention mechanism must be distinctly different.

The kinetic parameters describe the path-dependent measures of solute transfer from mobile to stationary phase. From the retention factor (Equation (1)), the rate constants from mobile to stationary phase ( $k_{sm}$ ) and from stationary to mobile phase ( $k_{ms}$ ) are defined by

$$k_{ms} = \frac{2kt_0}{\tau^2} \quad (5)$$

$$k_{sm} = k k_{ms} = \frac{2k^2t_0}{\tau^2} \quad (6)$$

where  $\tau^2$  is the variance arising from slow kinetics.<sup>[10,15]</sup> During the transfer between the mobile and stationary phases, the solute passes through a short-lived, high-energy transition state ( $\ddagger$ ). The Arrhenius equation is used to calculate the associated kinetic parameters

$$\ln k_{sm} = \ln A_{\ddagger m} - \frac{\Delta E_{\ddagger m}}{RT} \quad (7)$$

$$\ln k_{ms} = \ln A_{\ddagger s} - \frac{\Delta E_{\ddagger s}}{RT} \quad (8)$$

where  $A_{\ddagger m}$  and  $A_{\ddagger s}$  are the pre-exponential factors and  $\Delta E_{\ddagger m}$  and  $\Delta E_{\ddagger s}$  are the activation energies. Thus,  $\Delta E_{\ddagger m}$  or  $\Delta E_{\ddagger s}$  can be calculated from the slope of a graph of  $\ln k_{sm}$  or  $\ln k_{ms}$ , respectively, versus  $1/T$  at constant pressure. The activation enthalpies ( $\Delta H_{\ddagger m}$ ,  $\Delta H_{\ddagger s}$ ) can be calculated as

$$\Delta H_{\ddagger m} = \Delta E_{\ddagger m} - RT + P\Delta V_{\ddagger m} \quad (9)$$

$$\Delta H_{\ddagger s} = \Delta E_{\ddagger s} - RT + P\Delta V_{\ddagger s} \quad (10)$$

Using a similar method to the thermodynamic equations,

$$\ln k_{sm} = \frac{(-\Delta E_{\ddagger m} + T\Delta S_{\ddagger m} - P\Delta V_{\ddagger m})}{RT} \quad (11)$$

$$\ln k_{ms} = \frac{(-\Delta E_{\ddagger s} + T\Delta S_{\ddagger s} - P\Delta V_{\ddagger s})}{RT} \quad (12)$$

the activation volumes ( $\Delta V_{\ddagger m}$  and  $\Delta V_{\ddagger s}$ ) are calculated from the slope of a graph of  $\ln k_{sm}$  or  $\ln k_{ms}$ , respectively, versus  $P$  at constant temperature.

In this traditional approach, the retention process is considered to be analogous to a simple chemical reaction. Hence, it is important to understand the meaning of the derived parameters. The thermodynamic parameters (retention factor, changes in molar enthalpy and molar volume) represent the weighted average for all possible states of the solute in the mobile and stationary phases. Accordingly, the kinetic parameters (rate constant, activation enthalpy, and activation volume) represent the weighted average of all possible paths between all possible states. The kinetic parameters are a lumped sum of all processes including slow diffusion in the mobile phase, stationary phase, and pores, slow interfacial mass transport, and slow adsorption and desorption. Although this thermodynamic and kinetic treatment is an overt simplification, it provides much information about the retention process.

## EXPERIMENTAL

### Solutes

Eighteen aromatic hydrocarbons have been chosen to investigate the effect of the length of alkyl chain and number of methyl substituents on the thermodynamics and kinetics of retention on porous graphitic carbon. The alkylbenzenes (Figure 1) were chosen as a homologous series to study the effects of methylene addition on retention. Benzene, ethylbenzene, propylbenzene, butylbenzene, pentylbenzene, and hexylbenzene were obtained from Aldrich. The methylbenzenes (Figure 2) were chosen as a homologous series to study the effects of methyl substituent addition on retention. Toluene, *o*-xylene,

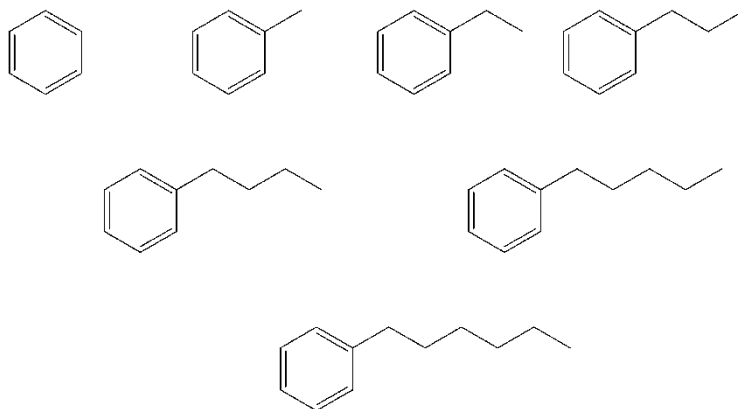


**Figure 1.** Structure of alkylbenzenes used to study retention on porous graphitic carbon.

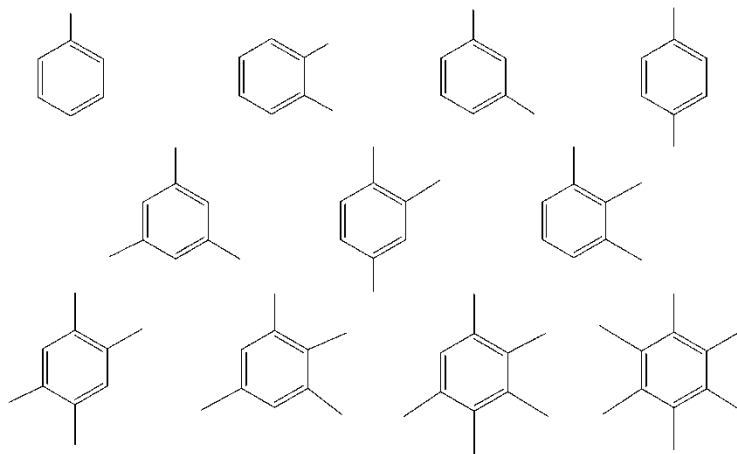


**Figure 2.** Structure of methylbenzenes used to study retention on porous graphitic carbon.

*m*-xylene, *p*-xylene, 1,2,3-trimethylbenzene, 1,2,4-trimethylbenzene, 1,3,5-trimethylbenzene, 1,2,3,5-tetramethylbenzene, 1,2,4,5-tetramethylbenzene, pentamethylbenzene, and hexamethylbenzene were obtained from Aldrich. Mixed standard solutions were prepared around  $10^{-3}$  M in high purity methanol (Burdick and Jackson, Baxter Healthcare) such that there was no overlap of solute zones at any temperature and pressure. A nonretained marker, acetonitrile, was added to each solution at a concentration of 1 M.

### Chromatographic System

The chromatographic system is shown schematically in Figure 3. It includes a single-piston reciprocating pump (Model 114 M, Beckman Instruments) operating in constant pressure mode ( $\pm 15$  psi) over the range of  $6.90 \times 10^6$  to  $3.45 \times 10^7$  Pa (1000 to 5000 psi). The pump allows for the mobile phase, methanol, to be supplied continuously without the need for depressurization during the refill cycle. At all pressures, the flow rate was maintained at approximately 1 mL/min at room temperature.

Samples are introduced by means of a manual injection valve (20  $\mu$ L, Model 7125, Rheodyne Instruments). Once the sample is introduced, it is carried by the methanol mobile phase to the column. The Hypercarb column is supplied by Shandon HPLC (100  $\times$  4.6 mm i.d., mean particle diameter 7  $\mu$ m). At the end of the column, a 100  $\mu$ m i.d. fused-silica capillary (Polymicro Technologies) is attached to serve as a restrictor. The length of the restrictor is reduced as the inlet pressure is decreased in order to maintain a constant pressure drop along the column ( $3.31 \times 10^5$  Pa/cm,

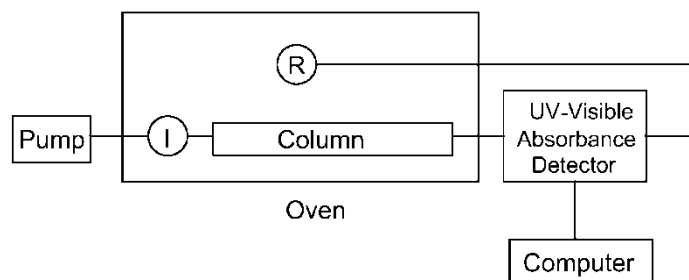


**Figure 3.** Schematic diagram of the chromatographic system. I = injector, R = restrictor.

48 psi/cm). The injector, column, and restrictor are all housed within an oven (Model SM900, Anspec Instruments) that maintains a constant temperature ( $\pm 0.1$  K) through the use of resistive heating coils. The oven was operated through the temperature range of 296 to 326 K.

The spectroscopic technique used for detection is ultraviolet-visible absorbance. As shown in Figure 3, a commercially available detector (Model UVIDEC-100-V, JASCO) is directly coupled to the column, such that the effluent is directed to a capillary flow cell. The flow cell is a transparent fused-silica capillary of 180  $\mu\text{m}$  i.d., able to hold high pressure in the chromatographic system. The wavelength for detection (210 nm) is chosen on the basis of the absorption maximum of the solutes and nonretained marker. The output from the detector is directed to a data acquisition board (Model PCIMIO-16XE50, National Instruments) and computer with associated software (Labview v3.1, National Instruments).

### Data Treatment and Analysis

After collection, the zone profile for each solute is extracted from the chromatogram using the previously established conditions for the minimum number of points, integration limits, and signal-to-noise ratio.<sup>[16]</sup> After extraction, the zone profiles are iteratively fit by nonlinear regression using a commercially available program (Peakfit v3.18, Jandel Scientific).

There are a variety of methods for the determination of thermodynamic and kinetic parameters from zone profiles.<sup>[9]</sup> Statistical moment methods are among the most common. However, the accuracy of the statistical moment calculation depends considerably upon the parameters noted above, particularly the integration limits and signal-to-noise ratio.<sup>[16–18]</sup> As a result of these limitations, nonlinear regression to the Gaussian, exponentially modified Gaussian (EMG), and other equations has been widely utilized.<sup>[9,19]</sup> The Gaussian and EMG equations provide fitting parameters that are directly related to the statistical moments and, hence, to the thermodynamic and



kinetic parameters. As a result, these equations were initially chosen to characterize the chromatographic zone profiles. Typically, the Gaussian equation produced nonrandom residuals with a relatively small value for the square of the correlation coefficient ( $R^2 = 0.968\text{--}0.988$ ). The EMG equation provided a significantly better fit with only small residuals around the maximum or end of the zone profiles. Moreover, the EMG equation yielded better statistical results than the Gaussian equation ( $R^2 = 0.992\text{--}0.999$ ). On the basis on these results, the EMG model was used throughout these studies. The EMG is a convolution of a Gaussian and an exponential function with the following form:

$$C(t) = \frac{A}{2\tau} \exp\left(\frac{\sigma^2}{2\tau^2} + \frac{t_G - t}{\tau}\right) \left( \operatorname{erf}\left(\frac{t - t_G}{\sqrt{2}\sigma} - \frac{\sigma}{\sqrt{2}\tau}\right) + 1 \right) \quad (13)$$

where  $A$  is the area,  $t_G$  is the mean of the Gaussian component,  $\sigma$  is the standard deviation of the Gaussian component, and  $\tau$  is the standard deviation of the exponential component. Thermodynamic parameters are derived from the first statistical moment or retention time, which is calculated as

$$t_r = t_G + \tau \quad (14)$$

and then substituted in Equation 1. Kinetic parameters are related to the second statistical moment, which is calculated as  $\sigma^2 + \tau^2$ . Zone broadening that arises from symmetrical processes is quantified by  $\sigma$ , whereas broadening that arises from asymmetrical processes is quantified by  $\tau$ . Asymmetric broadening may arise from several sources within the chromatographic system, including volumetric (e.g. injectors, unions, etc.), electronic (e.g. amplifiers), and physico-chemical processes (e.g. nonlinear isotherms, kinetics, etc.). The asymmetry that arises from instrumental sources can be minimized by careful experimental design, which is verified by negligible asymmetry of the nonretained marker. Thus, the kinetics of retention can be determined from the exponential variance after ensuring that the solute concentration is within the linear range of the isotherm. The kinetic parameters can then be calculated from Equations (5) and (6). The accuracy and precision of thermodynamic and kinetic parameters determined in this manner have been evaluated in previous work.<sup>[10,11]</sup>

## RESULTS AND DISCUSSION

Alkyl-substituted benzenes were chosen as the solutes for two reasons. First, they comprise a homologous series that is useful to establish trends in thermodynamic and kinetic behavior. Second, these solutes are of great environmental importance. BTEX is the collective name of benzene, toluene, ethylbenzene, and the xylene isomers. BTEX compounds are the most common aromatic compounds in petroleum, and are widely used in the manufacture of paints, synthetic rubber, and agricultural chemicals.<sup>[20]</sup> BTEX in petroleum can directly affect the physical and chemical

properties,<sup>[20]</sup> and can frequently enter soil, sediments, and groundwater because of accidental oil spills, leakage of gasoline and other petroleum fuels, and improper waste disposal practices. BTEX are hazardous carcinogenic and neurotoxic compounds and are classified as priority pollutants regulated by the U.S. Environment Protection Agency.<sup>[21]</sup>

### Thermodynamic Behavior

#### Retention Factor

By using Equation (1), the retention factor for each solute was calculated on PGC using a methanol mobile phase. The results of these calculations are summarized in Tables 1 and 2. For the homologous series of alkylbenzenes (Table 1), the retention factor increases with alkyl chain length at all temperatures and pressures. Solute with longer alkyl chains are more retained due to increased dispersion forces of the methylene groups with the stationary phase. The only exceptions are toluene and ethylbenzene, which produce very similar retention factors. This may be due to the greater effect on retention produced by an independent methyl substituent, which is discussed below.

The effect of temperature on the retention factor is very pronounced on porous graphitic carbon. For all alkylbenzenes, an increase in temperature results in a decrease in the retention factor. Solute with longer alkyl chains

**Table 1.** Retention factors ( $k$ ) and kinetic rate constants ( $k_{ms}$ ,  $k_{sm}$ ) for alkylbenzenes on porous graphitic carbon

Solute	$k^a$	$k^b$	$\Delta k/k$ (%) <sup>c</sup>	$k^d$	$k^e$	$\Delta k/k$ (%) <sup>f</sup>	$k_{ms}$ (s <sup>-1</sup> ) <sup>g</sup>	$k_{sm}$ (s <sup>-1</sup> ) <sup>h</sup>
Benzene	0.16	0.16	-4.9	0.16	0.16	1.9	5.9	1.0
Toluene	0.36	0.31	-16	0.34	0.33	-1.2	13	4.9
Ethylbenzene	0.37	0.30	-17	0.34	0.33	-0.9	12	4.5
Propylbenzene	0.53	0.43	-18	0.49	0.49	-0.4	15	8.4
Butylbenzene	0.80	0.62	-23	0.71	0.71	-0.1	17	14
Pentylbenzene	1.43	1.04	-28	1.23	1.24	1.3	16	24
Hexylbenzene	2.34	1.56	-33	1.90	1.93	1.5	15	37

<sup>a</sup>Retention factor calculated at  $T = 298$  K and  $P = 3.28 \times 10^7$  Pa (4760 psi).

<sup>b</sup>Retention factor calculated at  $T = 326$  K and  $P = 3.28 \times 10^7$  Pa (4760 psi).

<sup>c</sup> $\Delta k/k$  (%) =  $100 \times (k^b - k^a)/k^a$ .

<sup>d</sup>Retention factor calculated at  $T = 309$  K and  $P = 5.24 \times 10^6$  Pa (760 psi).

<sup>e</sup>Retention factor calculated at  $T = 309$  K and  $P = 3.28 \times 10^7$  Pa (4760 psi).

<sup>f</sup> $\Delta k/k$  (%) =  $100 \times (k^e - k^d)/k^d$ .

<sup>g</sup>Rate constants for the stationary to mobile phase transfer at  $T = 295$  K and  $P = 5.24 \times 10^6$  Pa (760 psi).

<sup>h</sup>Rate constants for the mobile to stationary phase transfer at  $T = 295$  K and  $P = 5.24 \times 10^6$  Pa (760 psi).

**Table 2.** Retention factors ( $k$ ) and kinetic rate constants ( $k_{ms}$ ,  $k_{sm}$ ) for methylbenzenes on porous graphitic carbon

Solute	$k^a$	$k^b$	$\Delta k/k$ (%) <sup>c</sup>	$k^d$	$k^e$	$\Delta k/k$ (%) <sup>f</sup>	$k_{ms}$ (s <sup>-1</sup> ) <sup>g</sup>	$k_{sm}$ (s <sup>-1</sup> ) <sup>h</sup>
Benzene	0.16	0.16	-4.9	0.16	0.16	1.9	5.9	1.0
Toluene	0.36	0.31	-16	0.34	0.33	-1.2	13	4.9
<i>o</i> -Xylene	0.99	0.75	-25	0.87	0.87	-0.2	14	14
<i>m</i> -Xylene	0.82	0.64	-22	0.73	0.73	-0.1	16	14
<i>p</i> -Xylene	0.96	0.72	-26	0.83	0.85	3.4	15	15
1,2,3-Trimethylbenzene	2.98	2.03	-32	2.48	2.50	0.9	14	45
1,2,4-Trimethylbenzene	2.52	1.72	-32	2.08	2.14	2.9	15	38
1,3,5-Trimethylbenzene	1.80	1.28	-29	1.52	1.55	1.8	20	38
1,2,3,5-Tetramethylbenzene	7.00	4.36	-38	5.53	5.63	1.7	3.5	25
1,2,4,5-Tetramethylbenzene	7.19	4.48	-38	5.69	5.88	3.4	16	121
Pentamethylbenzene	24.5	15.2	-38	20.5	20.9	1.8	3.5	99
Hexamethylbenzene	100	50.9	-49	71.0	74.8	5.3	2.7	292

<sup>a</sup>Retention factor calculated at T = 298 K and P =  $3.28 \times 10^7$  Pa (4760 psi).

<sup>b</sup>Retention factor calculated at T = 326 K and P =  $3.28 \times 10^7$  Pa (4760 psi).

<sup>c</sup> $\Delta k/k$  (%) =  $100 \times (k^b - k^a)/k^a$ .

<sup>d</sup>Retention factor calculated at T = 309 K and P =  $5.24 \times 10^6$  Pa (760 psi).

<sup>e</sup>Retention factor calculated at T = 309 K and P =  $3.28 \times 10^7$  Pa (4760 psi).

<sup>f</sup> $\Delta k/k$  (%) =  $100 \times (k^e - k^d)/k^d$ .

<sup>g</sup>Rate constants for the stationary to mobile phase transfer at T = 295 K and P =  $5.24 \times 10^6$  Pa (760 psi).

<sup>h</sup>Rate constants for the mobile to stationary phase transfer at T = 295 K and P =  $5.24 \times 10^6$  Pa (760 psi).

demonstrate a greater change in retention factor ( $\Delta k/k$ ), ranging from  $-4.9\%$  for benzene to  $-33\%$  for hexylbenzene for temperatures from 298 to 326 K. In contrast, the effect of pressure is much smaller on PGC. The change in retention factor for all alkylbenzenes typically ranges from  $-1.2\%$  to  $1.9\%$  for pressures from  $5.24 \times 10^6$  to  $3.28 \times 10^7$  Pa (760 to 4760 psi). This change is not statistically significant, considering the error in the measurement.

For the homologous series of methylbenzenes (Table 2), the retention factor increases with the number of methyl substituents at all temperatures and pressures. Solutes with more methyl substituents are more retained due to increased dispersion forces, as well as increased electron density of the phenyl ring arising from the electron-donating methyl groups. Each group of positional isomers produces similar retention factors. For example, the xylene isomers have similar retention factors at the same temperature and pressure. However, *m*-xylene is least retained because it has the lowest electron density of the phenyl ring among the isomers. Likewise, the trimethylbenzene isomers have similar retention factors, but 1,3,5-trimethylbenzene is the least retained for the same reasons. The tetramethylbenzene isomers also have similar retention factors.

The effect of temperature on the retention factor again is very pronounced. For all methylbenzenes, an increase in temperature results in a decrease in the retention factor. Solutes with more methyl substituents demonstrate a greater change of retention factor, ranging from  $-4.9\%$  for benzene to  $-49\%$  for hexamethylbenzene for temperatures from 298 to 326 K. In contrast, the effect of pressure is again much smaller on PGC. The retention factors for all methylbenzenes change very little with pressure, typically  $-1.2\%$  to  $5.3\%$  for pressures from  $5.24 \times 10^6$  to  $3.28 \times 10^7$  Pa (760 to 4760 psi).

Comparing the retention factors between the alkylbenzene and methylbenzene series, it can be concluded that the addition of a methyl group produces a greater effect on retention than a methylene group. This is because the methyl group can change the electron density of the phenyl ring to a greater extent than the methylene group. Furthermore, the methyl groups are a serial addition at different points of attachment, which will further increase retention, whereas the methylene groups are a serial addition at the same point of attachment.

### Molar Enthalpy

By using Equation (2), the change in molar enthalpy was calculated. A representative graph used in the calculation of the change in molar enthalpy is shown in Figure 4. For all solutes at all pressures, the data are linear ( $R^2 = 0.973\text{--}0.999$ ) and the slope of the line is positive. A linear graph indicates that the change in molar enthalpy is constant with temperature. A positive slope is demonstrative of a negative change in molar enthalpy, which indicates that the transition from the mobile to stationary phase is an

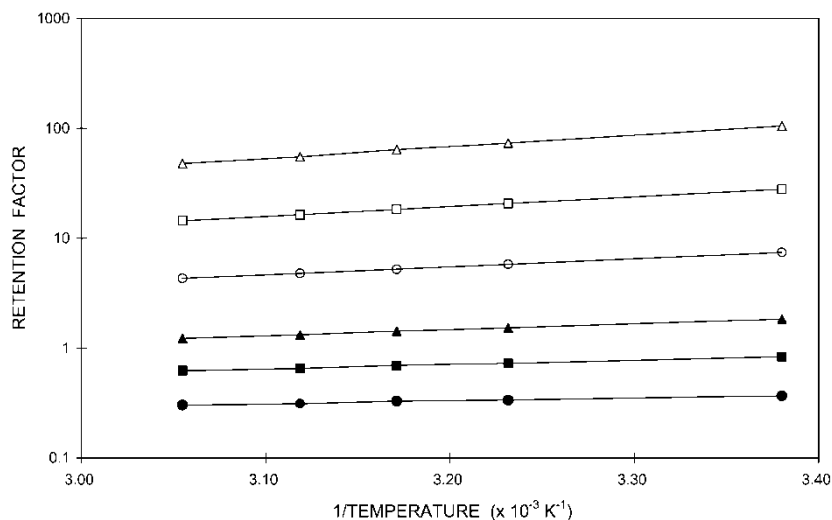


**Figure 4.** Representative graph of the logarithm of retention factor versus inverse temperature used to calculate the change in molar enthalpy according to Equation (2). Column: porous graphitic carbon,  $100 \times 4.6$  mm i.d.,  $7 \mu\text{m}$  particle size. Mobile phase: methanol,  $1.21 \times 10^7$  Pa (1760 psi), 0.955 mL/min. Solutes: toluene ( $\bullet$ ), *m*-xylene ( $\blacksquare$ ), 1,3,5-trimethylbenzene ( $\blacktriangle$ ), 1,2,4,5-tetramethylbenzene ( $\circ$ ), pentamethylbenzene ( $\square$ ), hexamethylbenzene ( $\triangle$ ).

energetically favorable exothermic process. Molar enthalpies for alkylbenzenes and methylbenzenes at different pressures are summarized in Tables 3 and 4.

The alkylbenzenes (Table 3) illustrate a trend of decreasing change in molar enthalpy, where retention becomes more exothermic as the number of methylene groups increases. The differential change in molar enthalpy ( $\Delta\Delta H$ ) versus carbon number for alkylbenzenes can be calculated. From benzene to toluene,  $\Delta H$  changes by about  $-3$  kJ/mol. But from toluene to propylbenzene, the change in  $\Delta H$  is very small at approximately  $-0.5$  kJ/mol. This small change suggests that the addition of one methylene group at this stage does not significantly affect the retention. Thereafter, the change in  $\Delta H$  becomes relatively constant at approximately  $-2$  kJ/mol. The change in molar enthalpy for alkylbenzenes with pressure is very small and statistically insignificant.

The methylbenzenes (Table 4) also illustrate a decreasing change in molar enthalpy as the number of methyl groups increases. Solutes with the same number of methyl substituents have similar changes in molar enthalpy. For example, the xylene isomers have comparable molar enthalpies of approximately  $-8$  kJ/mol. The same is true for the trimethylbenzene isomers, with molar enthalpies of approximately  $-11$  kJ/mol, and the tetramethylbenzene isomers, with molar enthalpies of approximately  $-14$  kJ/mol. The differential

**Table 3.** Molar enthalpy ( $\Delta H$ ) and molar volume ( $\Delta V$ ) for alkylbenzenes on porous graphitic carbon

Solute	$\Delta H$ (kJ/mol) <sup>a</sup>	$\Delta H$ (kJ/mol) <sup>b</sup>	$\Delta V$ (cm <sup>3</sup> /mol) <sup>c</sup>	$\Delta V$ (cm <sup>3</sup> /mol) <sup>d</sup>
Benzene	-2.3 ± 0.8	-1.6 ± 0.2	-0.2 ± 0.2	0.2 ± 0.2
Toluene	-5.1 ± 0.5	-5.0 ± 0.3	0.3 ± 0.2	0.2 ± 0.1
Ethylbenzene	-5.6 ± 0.5	-5.4 ± 0.4	0.2 ± 0.2	-0.3 ± 0.2
Propylbenzene	-5.8 ± 0.3	-5.7 ± 0.4	-0.4 ± 0.2	0.3 ± 0.2
Butylbenzene	-7.6 ± 0.4	-7.3 ± 0.3	0.2 ± 0.2	0.3 ± 0.2
Pentylbenzene	-9.4 ± 0.3	-9.1 ± 0.3	-0.3 ± 0.2	0.4 ± 0.3
Hexylbenzene	-11.7 ± 0.4	-11.2 ± 0.4	0.3 ± 0.3	-0.2 ± 0.2

<sup>a</sup>Molar enthalpy ( $\Delta H$ ) calculated at T = 295 to 327 K and P = 5.24 × 10<sup>6</sup> Pa (760 psi).

<sup>b</sup>Molar enthalpy ( $\Delta H$ ) calculated at T = 297 to 326 K and P = 3.28 × 10<sup>7</sup> Pa (4760 psi).

<sup>c</sup>Molar volume ( $\Delta V$ ) calculated at T = 296 K and P = 5.24 × 10<sup>6</sup> to 3.28 × 10<sup>7</sup> Pa (760 to 4760 psi).

<sup>d</sup>Molar volume ( $\Delta V$ ) calculated at T = 327 K and P = 5.24 × 10<sup>6</sup> to 3.28 × 10<sup>7</sup> Pa (760 to 4760 psi).

**Table 4.** Molar enthalpy ( $\Delta H$ ) and molar volume ( $\Delta V$ ) for methylbenzenes on porous graphitic carbon

Solute	$\Delta H$ (kJ/mol) <sup>a</sup>	$\Delta H$ (kJ/mol) <sup>b</sup>	$\Delta V$ (cm <sup>3</sup> /mol) <sup>c</sup>	$\Delta V$ (cm <sup>3</sup> /mol) <sup>d</sup>
Benzene	-2.3 ± 0.8	-1.6 ± 0.2	-0.2 ± 0.2	0.2 ± 0.2
Toluene	-5.1 ± 0.5	-5.0 ± 0.3	0.3 ± 0.2	0.2 ± 0.1
<i>o</i> -Xylene	-8.2 ± 0.2	-7.9 ± 0.3	0.3 ± 0.2	-0.2 ± 0.2
<i>m</i> -Xylene	-7.7 ± 0.5	-7.1 ± 0.4	-0.4 ± 0.2	0.2 ± 0.2
<i>p</i> -Xylene	-8.3 ± 0.3	-8.6 ± 0.3	0.2 ± 0.2	0.2 ± 0.2
1,2,3-Trimethylbenzene	-11.1 ± 0.1	-10.9 ± 0.2	0.3 ± 0.2	-0.4 ± 0.3
1,2,4-Trimethylbenzene	-11.1 ± 0.2	-10.8 ± 0.2	0.3 ± 0.3	0.2 ± 0.2
1,3,5-Trimethylbenzene	-10.1 ± 0.1	-9.6 ± 0.2	-0.3 ± 0.2	0.3 ± 0.2
1,2,3,5-Tetramethylbenzene	-13.6 ± 0.1	-13.3 ± 0.3	0.4 ± 0.3	-0.5 ± 0.4
1,2,4,5-Tetramethylbenzene	-13.9 ± 0.2	-13.4 ± 0.1	0.3 ± 0.2	0.4 ± 0.2
Pentamethylbenzene	-16.5 ± 0.3	-15.6 ± 0.1	-0.6 ± 0.2	0.6 ± 0.4
Hexamethylbenzene	-20.1 ± 0.4	-19.6 ± 0.4	0.6 ± 0.3	0.7 ± 0.3

<sup>a</sup>Molar enthalpy ( $\Delta H$ ) calculated at T = 295 to 327 K and P = 5.24 × 10<sup>6</sup> Pa (760 psi).

<sup>b</sup>Molar enthalpy ( $\Delta H$ ) calculated at T = 297 to 326 K and P = 3.28 × 10<sup>7</sup> Pa (4760 psi).

<sup>c</sup>Molar volume ( $\Delta V$ ) calculated at T = 296 K and P = 5.24 × 10<sup>6</sup> to 3.28 × 10<sup>7</sup> Pa (760 to 4760 psi).

<sup>d</sup>Molar volume ( $\Delta V$ ) calculated at T = 327 K and P = 5.24 × 10<sup>6</sup> to 3.28 × 10<sup>7</sup> Pa (760 to 4760 psi).

change in molar enthalpy versus carbon number for the methylbenzenes is relatively constant at around  $-2.5$  kJ/mol. This value is slightly larger than that for the alkylbenzenes when the carbon number is greater than three. The constant change suggests that the addition of each methyl group produces a similar effect on retention. The methylbenzenes also demonstrate very small differences in molar enthalpy at different pressures.

To understand the mobile phase contribution to these trends, the excess enthalpies for some solutes were estimated from the literature.<sup>[22,23]</sup> For the first three solutes in the alkylbenzene series, benzene has the smallest and ethylbenzene the largest excess enthalpy. For example, the excess enthalpies for benzene, toluene, and ethylbenzene are 0.0783, 0.0885, and 0.117 kJ/mol, respectively, at a mole fraction of 0.052 in methanol.<sup>[22]</sup> As the mole fraction decreases, toluene and ethylbenzene approach very similar excess enthalpies. These trends are consistent with those reported herein, where benzene exhibits the smallest absolute value of molar enthalpy, while toluene and ethylbenzene are larger and relatively comparable. For the xylene series, *o*- and *m*-xylene have very similar excess enthalpies, whereas *p*-xylene has a smaller value. For example, the excess enthalpies for *o*-, *m*-, and *p*-xylenes are 0.139, 0.133, and 0.125 kJ/mol, respectively, at a mole fraction of 0.056 in methanol.<sup>[23]</sup> These trends are not consistent with those reported herein, where *m*-xylene has the smallest absolute value of the molar enthalpy and *o*- and *p*-xylene are larger and relatively comparable. Hence, the mobile phase contributions can account for the general trends of increasing molar enthalpy with increasing number of methylene and methyl groups, but cannot account for the variations of positional isomers. These variations are more likely attributable to specific interactions with the graphitic surface.

To understand the stationary phase contribution to these trends, it is helpful to compare with octadecylsilica stationary phases. For low-density monomeric octadecylsilica, the change in molar enthalpy ( $\Delta H$ ) ranges from  $-7.3$  to  $-17.6$  kJ/mol for fatty acids  $C_{10}$  to  $C_{22}$ , respectively, at 303 K and  $9.17 \times 10^6$  Pa (1330 psi). The differential change in molar enthalpy per methylene group ( $\Delta\Delta H$ ) remains relatively constant, with an average value of  $-1.3$  kJ/mol.<sup>[24]</sup> For high-density polymeric octadecylsilica, the change in molar enthalpy ranges from  $-44$  to  $-128$  kJ/mol for fatty acids  $C_{10}$  to  $C_{22}$ , respectively, at 303 K and  $1.01 \times 10^7$  Pa (1470 psi).<sup>[24]</sup> The differential change in molar enthalpy per methylene group remains constant, with an average value of  $-3.9$  kJ/mol (24). Thus, the change in molar enthalpy on PGC is intermediate between those of low-density monomeric and high-density polymeric octadecylsilicas.

### Molar Volume

Similar to the molar enthalpy, the molar volume also provides insight into the effects that arise from structure. By using Equation (3), the change in molar volume was calculated. A representative graph used in the calculation of the change in molar volume is depicted in Figure 5. For all solutes at all

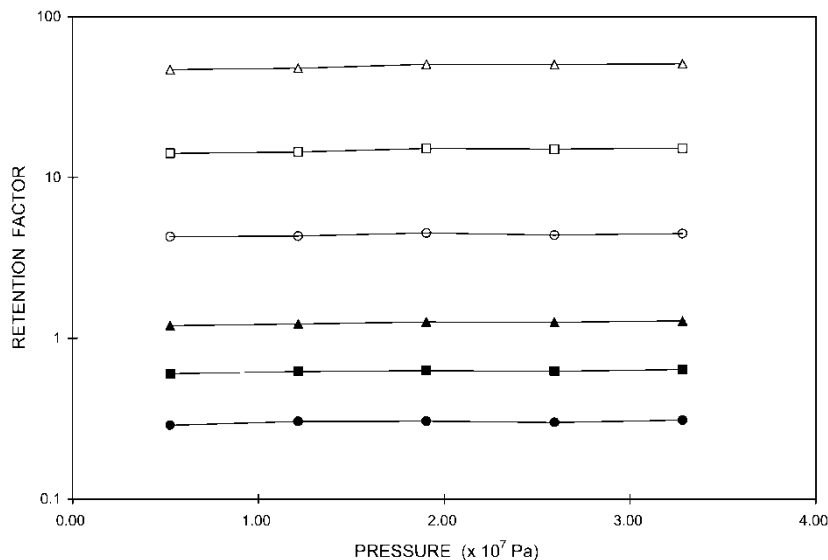


**Figure 5.** Representative graph of the logarithm of retention factor versus pressure used to calculate the change in molar volume according to Equation (3). Column: porous graphitic carbon,  $100 \times 4.6$  mm i.d.,  $7 \mu\text{m}$  particle size. Mobile phase: methanol, 327 K, 1.38 mL/min. Solutes: toluene ( $\bullet$ ), *m*-xylene ( $\blacksquare$ ), 1,3,5-trimethylbenzene ( $\blacktriangle$ ), 1,2,4,5-tetramethylbenzene ( $\circ$ ), pentamethylbenzene ( $\square$ ), hexamethylbenzene ( $\triangle$ ).

temperatures, the data are relatively linear. However, because of the small change in retention factor with pressure, the square of the correlation coefficient is small ( $R^2 = 0.549\text{--}0.889$ ). A linear graph indicates that the molar volume is constant with pressure. The slope of the line is slightly positive or negative. A negative slope results in a positive change in molar volume, which indicates that the solute occupies more space in the stationary phase than in the mobile phase. Conversely, a positive slope indicates that the solute transfer from the mobile to stationary phase results in a smaller volume. Representative data for the alkylbenzenes and methylbenzenes are contained in Tables 3 and 4.

Overall, the change in molar volume is very small on PGC. Considering the uncertainty in measurement, the change in molar volume is very close to zero. This is consistent with the retention mechanism on PGC, which is based on adsorption and desorption of the solute molecules from the solid stationary surface, rather than partition of the solute molecules into the stationary phase as on octadecylsilica. The change in molar volume for methylene homologues on low-density monomeric octadecylsilica ranges from 1.9 to  $-4.3 \text{ cm}^3/\text{mol}$ ,<sup>[24]</sup> which is greater than that on PGC. The change in molar volume for methylene homologues on high-density polymeric octadecylsilica ranges from  $-27$  to  $-104 \text{ cm}^3/\text{mol}$ ,<sup>[24]</sup> which is much greater than that on PGC.



## Enthalpy-Entropy Compensation

More detailed information about the retention process can be obtained from enthalpy-entropy compensation. As shown in Equation (4), a graph of the logarithm of the retention factor versus the negative change in molar enthalpy for a homologous series can be used to evaluate enthalpy-entropy compensation. Representative graphs for the alkylbenzenes and methylbenzenes are shown in Figures 6 and 7. It is apparent that these graphs are linear ( $R^2 = 0.985-0.987$ ), which confirms that enthalpy-entropy compensation occurs for both homologous series. However, the slopes of these graphs, which are related to the compensation temperatures, are distinctly different. The compensation temperature for the alkylbenzenes is determined to be 1050 K, whereas that for the methylbenzenes is 3400 K. The compensation temperature represents the ratio of the differential changes in molar enthalpy and molar entropy ( $T_c = \Delta\Delta H/\Delta\Delta S$ ). Hence, the large magnitude of these values suggests that the retention process is strongly dominated by enthalpic contributions. This predominance is clearly more significant for the methyl group (methylbenzenes) than for the methylene group (alkylbenzenes). The positive sign of the compensation temperatures suggests that the signs of  $\Delta\Delta H$  and  $\Delta\Delta S$  are the same. Given that  $\Delta\Delta H$  is negative, as

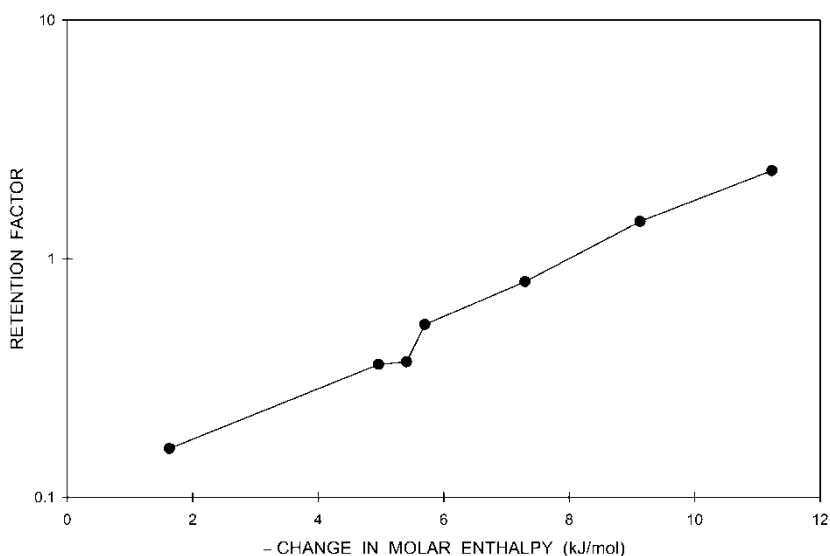


**Figure 6.** Representative graph of the logarithm of retention factor versus the negative change in molar enthalpy used to evaluate enthalpy-entropy compensation according to Equation (4). Column: porous graphitic carbon,  $100 \times 4.6$  mm i.d.,  $7 \mu\text{m}$  particle size. Mobile phase: methanol, 297 to 326 K,  $3.28 \times 10^7$  Pa (4760 psi). Solutes: alkylbenzenes.

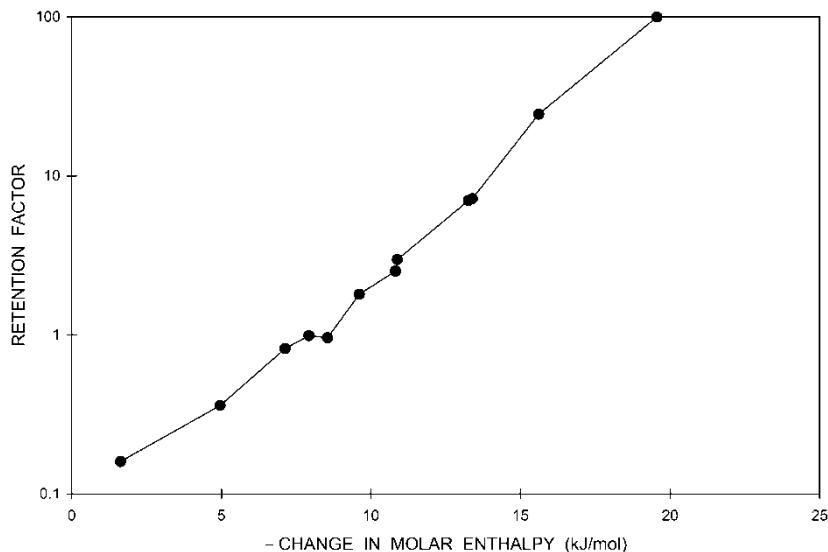


**Figure 7.** Representative graph of the logarithm of retention factor versus the negative change in molar enthalpy used to evaluate enthalpy-entropy compensation according to Equation (4). Column: porous graphitic carbon,  $100 \times 4.6$  mm i.d.,  $7 \mu\text{m}$  particle size. Mobile phase: methanol, 297 to 326 K,  $3.28 \times 10^7$  Pa (4760 psi). Solutes: methylbenzenes.

discussed above, this implies that  $\Delta\Delta S$  is also negative. Thus, the favorable changes in molar enthalpy are compensated by unfavorable changes in molar entropy for both homologous series. However, the disparate values for the compensation temperatures suggest that the retention mechanism is distinctly different for the methylene and methyl groups on PGC.

These compensation temperatures for PGC are significantly larger than those for octadecylsilica. The compensation temperature for methylene homologues on low-density monomeric octadecylsilica is 750 K, whereas that on high-density polymeric octadecylsilica is 330 K.<sup>[25]</sup> Hence, the enthalpic component is more important on PGC than on octadecylsilica and the retention mechanism is distinctly different.

### Kinetic Behavior

Although the thermodynamic data demonstrate the steady-state aspects, they do not fully explain the mechanism of retention. Using Equations (5–12), the pseudo-first-order rate constants, activation enthalpies, and activation volumes were calculated. These values help to quantify the kinetic aspects of solute transfer between the mobile and stationary phases.

## Rate Constants

Representative values of the rate constants are summarized in Tables 1 and 2. For the alkylbenzenes (Table 1), generally the molecules with a greater number of methylene groups exhibit larger rate constants for the mobile to stationary phase ( $k_{sm}$ ) and stationary to mobile phase ( $k_{ms}$ ) transitions. From benzene to butylbenzene, the rate limiting step is the transfer from mobile to stationary phase (i.e.,  $k_{ms} > k_{sm}$ ) because the retention factor, which is the ratio of  $k_{sm}$  and  $k_{ms}$ , is less than unity. However, for pentylbenzene and hexylbenzene, the rate limiting step is the transfer from stationary to mobile phase (i.e.,  $k_{ms} < k_{sm}$ ) because the retention factor is greater than unity.

For the methylbenzenes (Table 2), generally the molecules with a greater number of methyl substituents produce larger rate constants for the mobile to stationary phase ( $k_{sm}$ ) and stationary to mobile phase ( $k_{ms}$ ) transitions. For benzene, toluene, and the xylenes, the rate limiting step is the transfer from mobile to stationary phase (i.e.,  $k_{ms} > k_{sm}$ ) because the retention factor is less than unity. But for the trimethylbenzenes, tetramethylbenzenes, penta-methylbenzene, and hexamethylbenzene, the rate limiting step is the transfer from stationary to mobile phase (i.e.,  $k_{ms} < k_{sm}$ ) because the retention factor is greater than unity.

In addition, an increase in temperature yields an increase in the rate constants for all molecules. For example, the rate constant ( $k_{ms}$ ) for hexylbenzene ranges from 15 to 33 s<sup>-1</sup> for temperatures from 295 to 327 K, respectively, at 5.24 × 10<sup>6</sup> Pa (760 psi). In contrast, an increase in pressure yields only slight changes. The rate constant ( $k_{ms}$ ) for hexylbenzene ranges from 24 to 20 s<sup>-1</sup> for pressures from 5.24 × 10<sup>6</sup> to 3.28 × 10<sup>7</sup> Pa (760 to 4760 psi), respectively, at 309 K.

Overall, the data for the alkylbenzenes and methylbenzenes on PGC indicate that the rate constants ( $k_{ms}$  and  $k_{sm}$ ) increase as the retention factor increases. This is the reverse order observed for the fatty acids on high-density polymeric octadecylsilica. For example, the retention factor for the fatty acids C<sub>10</sub> to C<sub>22</sub> ranges from 0.56 to 67.3, respectively, whereas  $k_{ms}$  ranges from 5.05 to 0.90 s<sup>-1</sup> and  $k_{sm}$  ranges from 9.08 to 0.013 s<sup>-1</sup>, respectively, at 298 K and 3.15 × 10<sup>7</sup> Pa (4570 psi).<sup>[11]</sup> More detailed understanding of the kinetic behavior of octadecylsilica has been provided by Miyabe and Guiochon.<sup>[26–29]</sup> For the alkylbenzenes, the contribution of external mass transfer was shown to exceed that of axial dispersion and intraparticle diffusion. The external mass transfer contribution, which involves the rate of mass transfer from the bulk mobile phase to the external surface of the stationary phase by diffusion, increases with molecular size (i.e., number of methylene groups). The intraparticle diffusion contribution was shown to arise primarily from surface diffusion, rather than from pore diffusion. The surface diffusion coefficient was calculated and was shown to be correlated with molecular size and equilibrium constant. Hence, the reported decrease

in rate constant with increasing retention factor or number of methylene groups for octadecylsilica<sup>[11]</sup> can be understood on the basis of these individual contributions to kinetic behavior. For PGC, more detailed studies will be necessary to fully elucidate the kinetic behavior.

### Activation Enthalpy

By using Equations (7–10), the activation enthalpies were calculated. Figure 8 illustrates a typical graph of the natural logarithm of the rate constant versus inverse temperature used in the calculation of the activation enthalpy. For all solutes at all pressures, the data are linear ( $R^2 = 0.443\text{--}0.869$ ) and the slope of the line is negative. A linear graph indicates that the activation enthalpy is constant with temperature. A negative slope is demonstrative of a positive activation enthalpy, which is the energy barrier for the transfer from mobile or stationary phase to the transition state. Tables 5 and 6 contain the activation enthalpies for the alkylbenzenes and methylbenzenes.

For the alkylbenzenes (Table 5), the activation enthalpy from the stationary phase to the transition state ( $\Delta H_{\ddagger s}$ ) increases with increasing number of methylene groups. This result suggests that the enthalpy barrier from the

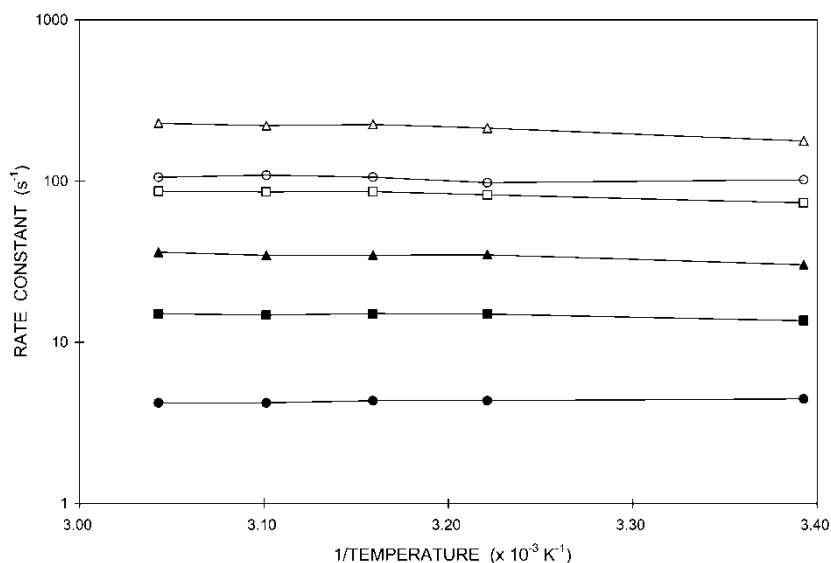


**Figure 8.** Representative graph of the logarithm of rate constant ( $k_{sm}$ ) versus inverse temperature used to calculate the activation enthalpy according to Equations (7) and (9). Column: porous graphitic carbon,  $100 \times 4.6$  mm i.d.,  $7 \mu\text{m}$  particle size. Mobile phase: methanol,  $1.90 \times 10^7$  Pa (2760 psi),  $0.956$  mL/min. Solutes: toluene ( $\bullet$ ), *m*-xylene ( $\blacksquare$ ), 1,3,5-trimethylbenzene ( $\blacktriangle$ ), 1,2,4,5-tetramethylbenzene ( $\circ$ ), pentamethylbenzene ( $\square$ ), hexamethylbenzene ( $\triangle$ ).

**Table 5.** Activation enthalpy ( $\Delta H_{\ddagger s}$ ,  $\Delta H_{\ddagger m}$ ) and activation volume ( $\Delta V_{\ddagger s}$ ,  $\Delta V_{\ddagger m}$ ) for alkylbenzenes on porous graphitic carbon

Solute	$\Delta H_{\ddagger s}$ (kJ/mol) <sup>a</sup>	$\Delta H_{\ddagger m}$ (kJ/mol)	$\Delta V_{\ddagger s}$ (cm <sup>3</sup> /mol) <sup>b</sup>	$\Delta V_{\ddagger m}$ (cm <sup>3</sup> /mol)
Benzene	3.7 ± 1.2	1.4 ± 0.9	-0.9 ± 0.9	0.9 ± 0.7
Toluene	6.9 ± 0.5	1.7 ± 0.4	1.2 ± 0.7	0.8 ± 0.9
Ethylbenzene	6.6 ± 1.2	0.8 ± 1.4	1.2 ± 1.0	-1.1 ± 0.9
Propylbenzene	8.4 ± 1.3	2.9 ± 1.1	1.4 ± 1.2	1.0 ± 0.7
Butylbenzene	10.8 ± 0.1	3.1 ± 0.5	1.3 ± 0.9	-1.3 ± 0.8
Pentylbenzene	11.4 ± 0.7	1.9 ± 1.2	-1.3 ± 0.8	1.0 ± 0.8
Hexylbenzene	13.8 ± 0.7	2.2 ± 0.7	1.3 ± 0.8	-0.8 ± 0.7

<sup>a</sup>Activation enthalpies from the stationary phase to transition state ( $\Delta H_{\ddagger s}$ ), and mobile phase to transition state ( $\Delta H_{\ddagger m}$ ) calculated at T = 295 to 327 K and P = 5.24 × 10<sup>6</sup> Pa (760 psi).

<sup>b</sup>Activation volumes from the stationary phase to transition state ( $\Delta V_{\ddagger s}$ ), and mobile phase to transition state ( $\Delta V_{\ddagger m}$ ) calculated at T = 296 K and P = 5.24 × 10<sup>6</sup> to 3.28 × 10<sup>7</sup> Pa (760 to 4760 psi).

**Table 6.** Activation enthalpy ( $\Delta H_{\ddagger s}$ ,  $\Delta H_{\ddagger m}$ ) and activation volume ( $\Delta V_{\ddagger s}$ ,  $\Delta V_{\ddagger m}$ ) for methylbenzenes on porous graphitic carbon

Solute	$\Delta H_{\ddagger s}$ (kJ/mol) <sup>a</sup>	$\Delta H_{\ddagger m}$ (kJ/mol)	$\Delta V_{\ddagger s}$ (cm <sup>3</sup> /mol) <sup>b</sup>	$\Delta V_{\ddagger m}$ (cm <sup>3</sup> /mol)
Benzene	3.7 ± 1.2	1.4 ± 0.9	-0.9 ± 0.9	0.9 ± 0.7
Toluene	6.9 ± 0.5	1.7 ± 0.4	1.2 ± 0.7	0.8 ± 0.9
<i>o</i> -Xylene	12.4 ± 1.0	4.2 ± 0.9	1.3 ± 1.0	-1.2 ± 1.2
<i>m</i> -Xylene	10.8 ± 2.2	2.1 ± 1.4	-1.4 ± 1.2	1.2 ± 1.2
<i>p</i> -Xylene	12.2 ± 1.8	3.8 ± 1.7	1.2 ± 1.2	-1.7 ± 1.2
1,2,3-Trimethylbenzene	13.8 ± 1.0	2.0 ± 0.9	-2.4 ± 1.8	1.3 ± 1.2
1,2,4-Trimethylbenzene	15.0 ± 1.6	3.9 ± 1.5	2.2 ± 2.2	-1.8 ± 1.5
1,3,5-Trimethylbenzene	14.9 ± 1.2	4.5 ± 1.1	2.3 ± 1.9	1.3 ± 1.2
1,2,3,5-Tetramethylbenzene	17.5 ± 0.7	3.9 ± 0.6	2.4 ± 2.3	-2.0 ± 1.7
1,2,4,5-Tetramethylbenzene	16.1 ± 1.1	2.2 ± 1.1	-2.1 ± 2.2	1.9 ± 1.9
Pentamethylbenzene	25.4 ± 1.5	8.5 ± 1.4	-2.6 ± 2.2	1.6 ± 1.5
Hexamethylbenzene	46.4 ± 8.9	26.1 ± 8.6	-2.5 ± 1.3	2.3 ± 2.3

<sup>a</sup>Activation enthalpies from the stationary phase to transition state ( $\Delta H_{\ddagger s}$ ), and mobile phase to transition state ( $\Delta H_{\ddagger m}$ ) calculated at T = 295 to 327 K and P = 5.24 × 10<sup>6</sup> Pa (760 psi).

<sup>b</sup>Activation volumes from the stationary phase to transition state ( $\Delta V_{\ddagger s}$ ), and mobile phase to transition state ( $\Delta V_{\ddagger m}$ ) calculated at T = 296 K and P = 5.24 × 10<sup>6</sup> to 3.28 × 10<sup>7</sup> Pa (760 to 4760 psi).

stationary phase to the transition state increases with the addition of each methylene group. The differential change in activation enthalpy ( $\Delta\Delta H_{\ddagger s}$ ) versus carbon number of the alkylbenzenes can be calculated. From benzene to toluene,  $\Delta\Delta H_{\ddagger s}$  is about 3 kJ/mol. But from toluene to propylbenzene,  $\Delta\Delta H_{\ddagger s}$  increases only slightly at 0.5 kJ/mol. When the carbon number is greater than three,  $\Delta\Delta H_{\ddagger s}$  is relatively constant at 2 kJ/mol, indicating that the effect of each methylene group on activation enthalpy is relatively constant.

For the methylbenzenes (Table 6), the activation enthalpy from the stationary phase to the transition state ( $\Delta H_{\ddagger s}$ ) increases with increasing number of methyl substituents. This result suggests that the enthalpy barrier from the stationary phase to the transition state increases with the addition of each methyl group. Solutes with the same number of methyl substituents have similar activation enthalpies. For example, *o*-, *m*-, and *p*-xylenes have comparable stationary phase to transition state activation enthalpies of approximately 12 kJ/mol. The differential change in activation enthalpy ( $\Delta\Delta H_{\ddagger s}$ ) versus carbon number of the methylbenzenes can also be calculated. From benzene to the tetramethylbenzenes, the differential change in activation enthalpy  $\Delta\Delta H_{\ddagger s}$  is relatively constant at around 3 kJ/mol. But for pentamethylbenzene and hexamethylbenzene,  $\Delta\Delta H_{\ddagger s}$  is greater than 8 kJ/mol.

For both alkylbenzenes and methylbenzenes, the activation enthalpy from the mobile phase to transition state ( $\Delta H_{\ddagger m}$ ) is nearly constant, considering the uncertainty in the kinetic data. But  $\Delta H_{\ddagger m}$  for pentamethylbenzene and hexamethylbenzene is greater than that of other solutes in the same homologous series. Comparison of the magnitude of  $\Delta H_{\ddagger m}$  and  $\Delta H_{\ddagger s}$  suggests that retention on PGC is predominantly controlled by the desorption process, which is dependent upon the molecular structure of the solutes. Hence, different molecules have different interaction with the stationary phase in the transition state, which affects the energy needed to transfer from stationary to mobile phases. Comparison of the activation enthalpies and the absolute value of the molar enthalpy reveals the following trend:  $\Delta H_{\ddagger s} > \Delta H > \Delta H_{\ddagger m}$ . As expected,  $\Delta H$  is nearly equal to the difference between  $\Delta H_{\ddagger s}$  and  $\Delta H_{\ddagger m}$ .

Again, it is instructive to compare the behavior of PGC and octadecylsilica. On the high-density polymeric octadecylsilica stationary phase,  $\Delta H_{\ddagger m}$  ranges from 3.96 to 2.21 kJ/mol and  $\Delta H_{\ddagger s}$  ranges from 7.54 to 11.0 kJ/mol for fatty acids C<sub>10</sub> to C<sub>22</sub>, respectively, at 303 K and  $3.15 \times 10^7$  Pa (4570 psi).<sup>[11]</sup> Hence, the activation enthalpies on PGC are comparable to those on octadecylsilica stationary phases.

### Activation Volume

By using Equations (11) and (12), the activation volumes from mobile phase to transition state ( $\Delta V_{\ddagger m}$ ) and from stationary phase to transition state ( $\Delta V_{\ddagger s}$ ) were calculated. A representative graph of the natural logarithm of the rate constant versus pressure is depicted in Figure 9 and resulting values for the activation

volume are presented in Tables 5 and 6. The slope of the line is either slightly positive or slightly negative. The activation volumes  $\Delta V_{\ddagger m}$  and  $\Delta V_{\ddagger s}$  appear to be larger than the change in molar volume ( $\Delta V$ ) because of greater uncertainty of the kinetic data. However, these values are also nearly zero. They are much smaller than the activation volumes reported for methylene and benzene homologues on high-density polymeric octadecylsilica.<sup>[11]</sup> For example,  $\Delta V_{\ddagger m}$  ranges from 7.2 to 110 cm<sup>3</sup>/mol and  $\Delta V_{\ddagger s}$  ranges from 31.7 to 211 cm<sup>3</sup>/mol for fatty acids C<sub>10</sub> to C<sub>22</sub>, respectively, at 303 K and  $2.76 \times 10^6$  to  $3.15 \times 10^7$  Pa (400 to 4570 psi).<sup>[11]</sup> This suggests that the volume barrier on PGC is much smaller than that on octadecylsilica stationary phases.

### Relationship Between Thermodynamic and Kinetic Behavior

Finally, it is beneficial to examine the relationship between the thermodynamic and kinetic behavior of the solutes. A priori, there is no expected relationship between the retention factor and the individual rate constants other than that given by Equation (6) ( $k = k_{sm}/k_{ms}$ ). In practice, however, there are three cases that are commonly observed for a closely related series

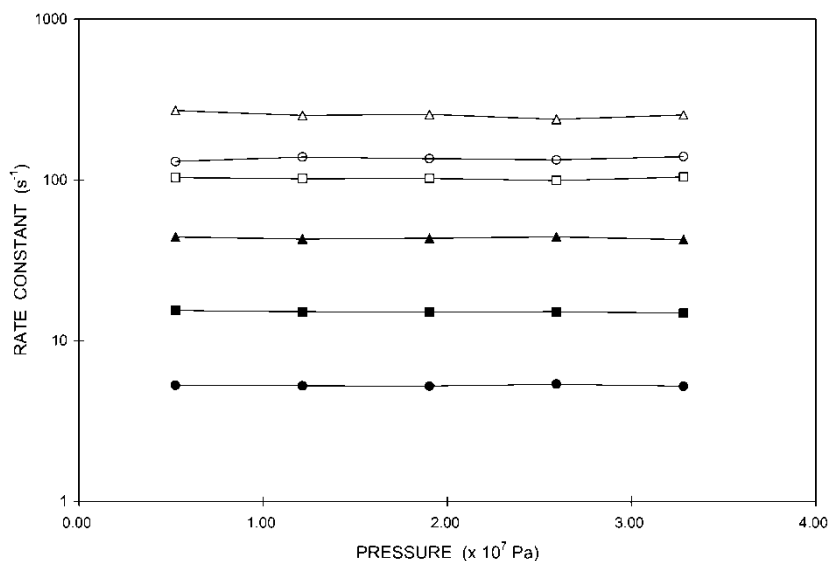


**Figure 9.** Representative graph of the logarithm of rate constant ( $k_{sm}$ ) versus pressure used to calculate the activation volume according to Equation (11). Column: porous graphitic carbon,  $100 \times 4.6$  mm i.d.,  $7 \mu\text{m}$  particle size. Mobile phase: methanol, 327 K, 1.38 mL/min. Solutes: toluene ( $\bullet$ ), *m*-xylene ( $\blacksquare$ ), 1,3,5-trimethylbenzene ( $\blacktriangle$ ), 1,2,4,5-tetramethylbenzene ( $\circ$ ), pentamethylbenzene ( $\square$ ), hexamethylbenzene ( $\Delta$ ).

of solutes.<sup>[30]</sup> In the first limiting case,  $k_{ms}$  is constant and  $k$  is linearly related to  $k_{sm}$ . In the second limiting case,  $k_{sm}$  is constant and  $k$  is inversely related to  $k_{ms}$ . In the third case,  $k$  varies with both  $k_{ms}$  and  $k_{sm}$  in a more complex manner. The data in Tables 1 and 2 provide the first information about this relationship for reversed-phase separations on PGC. For most of the solutes, both alkylbenzenes and methylbenzenes, the first limiting case applies: the rate of transfer from stationary to mobile phase is relatively constant. The rate of transfer from mobile to stationary phase increases with the retention factor, perhaps due to greater cohesive attraction with increasing number of methylene or methyl groups. There is some deviation from this behavior for the most highly substituted methylbenzenes, which seem to have a more complex relationship where both  $k_{ms}$  and  $k_{sm}$  vary as in the third case.

## CONCLUSIONS

In the research presented in this paper, solute transfer of two series of aromatic hydrocarbons (alkylbenzenes and methylbenzenes) has been studied as a function of molecular structure. By quantitating the thermodynamics and kinetics together, a better description of retention on PGC is made, providing a more accurate comparison of different solutes and stationary phases.

In the thermodynamic studies, the retention factor of alkylbenzenes increases with increasing number of methylene groups, and the retention factor of methylbenzenes increases with increasing number of methyl substituents. For the same solute, the retention factor decreases with an increase in temperature, but does not change significantly with pressure. The data from this study indicate that increases in the number of methylene and methyl groups result in more negative changes in molar enthalpy ( $\Delta H$ ). The more negative change in  $\Delta H$  suggests that the transition from mobile to stationary phase is a more energetically favorable exothermic process with each methylene or methyl group added. Enthalpy-entropy compensation is observed for both homologous series, and the compensation temperatures suggest that the retention mechanism is strongly dominated by enthalpic contributions. The data also show that the change in molar volume ( $\Delta V$ ) is close to zero, which indicates that the solute molecules adsorb on the surface of PGC instead of penetrating further into the stationary phase, as in octadecylsilica.

In the kinetic studies, the rate constants of alkylbenzenes and methylbenzenes increase with increasing number of methylene and methyl groups. The enthalpic barriers between the stationary phase and transition state ( $\Delta H_{\ddagger,s}$ ) were found to increase with increasing number of methylene and methyl groups. However, the enthalpic barriers between the mobile phase and transition state ( $\Delta H_{\ddagger,m}$ ) were much smaller than  $\Delta H_{\ddagger,s}$  and, at the same time, were very similar for all the solutes. The enthalpic barriers suggest that retention on PGC is controlled by the desorption of solutes from the stationary



phase. The volumetric barriers  $\Delta V_{\ddagger s}$  and  $\Delta V_{\ddagger m}$  again are very close to zero, owing to the adsorption mechanism on porous graphitic carbon.

## REFERENCES

1. Knox, J.H.; Kaur, B.; Millward, G.R. Structure and performance of porous graphitic carbon in liquid chromatography. *J. Chromatogr.* **1986**, *352*, 3–25.
2. Knox, J.H.; Ross, P. Carbon-based packing materials for liquid chromatography. Structure, performance, and retention mechanisms. *Adv. Chromatogr.* **1997**, *37*, 73–119.
3. Hennion, M.C.; Coquart, V.; Guenu, S.; Sella, C. Retention behavior of polar compounds using porous graphitic carbon with water-rich mobile phases. *J. Chromatogr. A* **1995**, *712*, 287–301.
4. Machtalere, G.; Pichon, V.; Hennion, M.C. Relationships between retention factors and analyte hydrophobicity on cyanopropyl and n-octadecyl bonded silicas, cross-linked polymers and porous graphitic carbon stationary phases. Consequences for the trace analysis of highly polar organic compounds. *J. High Resol. Chromatogr.* **2000**, *23*, 437–444.
5. Hennion, M.C. Ecole Supérieure de Physique et de Chimie Industrielles (ESPCI), private communication, 2003.
6. Pietrogrande, M.C.; Benvenuti, A.; Previato, S.; Dondi, F. HPLC analysis of PCBs on porous graphitic carbon: retention behavior and gradient elution. *Chromatographia* **2000**, *52*, 425–432.
7. Kriz, J.; Adamcova, E.; Knox, J.H.; Hora, J. Characterization of adsorbents by high-performance liquid chromatography using aromatic hydrocarbons. Porous graphite and its comparison with silica gel, alumina, octadecylsilica and phenylsilica. *J. Chromatogr. A* **1994**, *663*, 151–161.
8. Wan, Q.H.; Shaw, P.N.; Davies, M.C.; Barrett, D.A. Chromatographic behavior of positional isomers on porous graphitic carbon. *J. Chromatogr. A* **1995**, *697*, 219–227.
9. Li, X.; Hupp, A.M.; McGuffin, V.L. The thermodynamic and kinetic basis of liquid chromatography. *Adv. Chromatogr.* **2006**, *45*, 1–88.
10. Howerton, S.B.; McGuffin, V.L. Thermodynamic and kinetic characterization of polycyclic aromatic hydrocarbons in reversed-phase liquid chromatography. *Anal. Chem.* **2003**, *75*, 3539–3548.
11. McGuffin, V.L.; Lee, C. Thermodynamics and kinetics of solute transfer in reversed-phase liquid chromatography. *J. Chromatogr. A* **2003**, *987*, 3–15.
12. Leffler, J.; Grunwald, E. *Rates and Equilibria of Organic Reactions*; Wiley: New York, NY, 1963.
13. Krug, R.R.; Hunter, W.G.; Grieger, R.A. Enthalpy-entropy compensation. 2. Separation of the chemical from the statistical effect. *J. Phys. Chem.* **1976**, *80*, 2341–2351.
14. Ranatunga, R.; Vitha, M.F.; Carr, P.W. Mechanistic implications of the equality of compensation temperatures in chromatography. *J. Chromatogr. A* **2002**, *946*, 47–49.
15. Giddings, J.C. *Dynamics of Chromatography*; Marcel Dekker: New York, NY, 1965.
16. Howerton, S.B.; Lee, C.; McGuffin, V.L. Additivity of statistical moments in the exponentially modified Gaussian model of chromatography. *Anal. Chim. Acta* **2003**, *478*, 99–110.

17. Chesler, S.N.; Cram, S.P. Effect of peak sensing and random noise on the precision and accuracy of statistical moment analyses from digital chromatographic data. *Anal. Chem.* **1971**, *43*, 1922–1929.
18. Schudel, J.V.H.; Guiochon, G. Effect of random noise and peak asymmetry on the precision and accuracy of measurements of the column efficiency in chromatography. *J. Chromatogr.* **1988**, *457*, 1–12.
19. Barber, W.E.; Carr, P.W. Graphical method for obtaining retention time and number of theoretical plates from tailed chromatographic peaks. *Anal. Chem.* **1981**, *53*, 1939–1942.
20. Atteia, O.; Franceschi, M. Kinetics of natural attenuation of BTEX: review of the critical conditions and measurements at bore scale. *The Scientific World Journal* **2002**, *2*, 1338–1346.
21. List of lists. U.S. Environmental Protection Agency, July 1987.
22. Srivastava, R.; Smith, B.D. Evaluation of binary excess enthalpy data for the methanol + hydrocarbon systems. *J. Phys. Chem. Ref. Data* **1987**, *16*, 219–237.
23. Letcher, T.M.; Prasad, A.K.; Schoonbaert, F.E.Z.; Mercer-Chalmers, J. Excess enthalpies of (a xylene + an alkanol) at 298.2K. *J. Chem. Thermodynamics* **1990**, *22*, 765–770.
24. McGuffin, V.L.; Chen, S.H. Molar enthalpy and molar volume of methylene and benzene homologues in reversed-phase liquid chromatography. *J. Chromatogr. A* **1997**, *762*, 35–46.
25. Chen, S.H. *Fundamental Studies of Chromatographic Systems using Fluorescence Spectroscopy*; Ph. D. Dissertation, Michigan State University, 1993.
26. Miyabe, K.; Takeuchi, S. Surface diffusion of alkylbenzenes on octadecylsilyl-silica gel. *Ind. Eng. Chem. Res.* **1998**, *37*, 1154–1158.
27. Miyabe, K.; Guiochon, G. Correlation between surface diffusion and molecular diffusion in reversed-phase liquid chromatography. *J. Phys. Chem. B* **2001**, *105*, 9202–9209.
28. Miyabe, K.; Guiochon, G. Analysis of the surface diffusion of alkylbenzenes and p-alkylphenols in reversed-phase liquid chromatography using the surface-restricted molecular diffusion model. *Anal. Chem.* **2001**, *73*, 3096–3106.
29. Miyabe, K.; Guiochon, G. A kinetic study of mass transfer in reversed-phase liquid chromatography on a C18-silica gel. *Anal. Chem.* **2000**, *72*, 5162–5171.
30. Steinfeld, J.I.; Francisco, J.S.; Hase, W.L. *Chemical Kinetics and Dynamics*; Prentice-Hall: Englewood Cliffs, NJ, 1989.

Received November 18, 2006

Accepted December 14, 2006

Manuscript 6901